Quasi one-dimensional Ag nanostructures on Si(331)–(12 × 1)

N. Mariotti [a,*], C. Didiot [a], E.F. Schwier [b], C. Monney [c], C. Battaglia [d], P. Aebi [a]

[a] Département de Physique and Fribourg Center for Nanomaterials, Université de Fribourg, Chemin du Musée 3, 1700 Fribourg, Switzerland
[b] Hiroshima Synchrotron Radiation Center, Hiroshima University, 2-313 Kagamiyama, Higashi, Hiroshima 739-0046, Japan
[c] Department of Physics, University of Zürich, Winterthurerstrasse 190, 8057 Zürich, Switzerland
[d] Empa, Materials for Energy Conversion, 8600 Dübendorf, Switzerland

We report on the deposition of sub-monolayer Ag on the Si(331)–(12 × 1) surface. The growth of one-dimensional Ag nanostructures is observed by means of low-temperature scanning tunneling microscopy and low energy electron diffraction. We find that the deposited Ag is organized in nanostructures consistently taking "sawtooth" shapes. While the structures are not perfectly organized, their back edges are atomically straight. The limitations of this system in terms of faceting are also discussed.

1. Introduction

One-dimensional (1D) nanostructures have recently attracted considerable attention [1]. For instance, 1D metallic nanowires are directly related to the question of conduction and connections at the nanoscale [2]. Because connection wires in electronic technology are close to reach fundamental limits, the study of conduction in extremely thin nanostructures is of technological importance. On the other hand, the confinement of electrons in 1D gives rise to new physical phenomena, which are interesting from the fundamental and technological points of view [3,4].

The case of metallic nanostructures on semiconductors is particularly important for electronics, due to decoupling of the electronic states of the wire and those of the bulk induced by the semiconductor gap. Au and Ag-induced atomic wires form on the Si(557) surface [5]. Recently, Pb chains on the Si(553)–Au surface have been studied [6]. The Si(557)–(1 × 2)–Au surface is a faceted reconstruction exhibiting the formation of quasi-1D structures having proximal bands close to the Fermi level [7]. As another example, evidences of Tomonaga–Luttinger liquid behavior have been found for self-organized Au atomic chains on Ge(001) [8,9].

The Si(331)–(12 × 1) surface studied here is interesting because it is the only stable reconstructed surface lying between the important Si(111) and Si(001) surfaces. A review of the surface reconstructions of Si and their building blocks has been written by Battaglia et al. [10]. A well ordered surface can be related to surface potential barriers that can, in turn, act as a template for the growth of nanostructures. Since it is possible to prepare the Si(331)–(12 × 1) surface with a very low defect density, the question of using it as a template for growth of nanostructures rises naturally.

Dolbak et al. have studied the deposition of Ag on a vicinal Si(111) surface, comprising Si(111) and Si(331) facets, by means of Low Energy Electron Diffraction (LEED) [11]. They observed that the Ag-covered Si(331) surface breaks down in the more stable Si(111) and Si(110) facets at about 825 K. The break down increases with Ag coverage and is complete at 1 ML Ag. This indicates a limitation for the growth of Ag nanostructures on this surface reconstruction.

To avoid faceting, we explored the deposition of Ag on the Si(331)–(12 × 1) surface at coverages below 0.3 ML. We observed with STM and LEED the effect of an increase in annealing temperature. After optimizing the preparation conditions, structures with a long-range, atomically-straight edge along the $[\bar{1}10]$ direction, were formed. We describe here their morphology as observed by STM at 77 K. After an annealing at 850 K, the surface starts to break down in facets having three typical orientations, close to the Si(331) orientation vector.

2. Experiments

We used n-doped silicon samples with a resistivity between 0.001 and 0.005 Ω cm. To prepare the Si(331)–(12 × 1) reconstruction, the samples were flashed three times at 1535 K to clean the surface by applying direct current. Then the samples were slowly cooled down across the transition temperature of the Si(331)–(12 × 1) reconstruction (1085 K). Temperature was monitored using a pyrometer. Silver was deposited with an e-beam evaporation cell while the Si sample was heated by a direct current at a temperature of 330 ± 50 °C. The

* Corresponding author.
E-mail address: nicolas.mariotti@unifr.ch (N. Mariotti).

chamber pressure during evaporation never exceeded $5 \cdot 10^{-10}$ mbar. The measurements were performed at 77 K with an Omicron LT-STM. LEED measurements were performed at room temperature.

3. Results and discussion

In Fig. 1a, we present images of the bare surface at a voltage bias of +2.5 V. All the voltage biases specified in the article are with respect to the STM tip. This means that the positive biases correspond to tunneling into unoccupied states of the sample. The rounded protrusions correspond to the pentamers, which were reported, along with an atomic structure model, by Battaglia et al. [12]. At this voltage bias, the pentamers already start to acquire a rhomboidal shape. It is possible to see that the protrusions are aligned in the double chain configuration; the chains are highlighted by dashed lines. Fig. 1b shows the double chains observed with the best conditions, i.e., at +2 V. The latter kind of images allowed to propose the pentamer double chains model for the Si(331)–(12 × 1) surface [12]. The dots highlight the positions of the pentamer atoms (the central atom is not visible as a protrusion) The chains run along the $[\bar{1}\bar{1}6]$ direction. The differences between images a and b could be explained as follows. Since the dominant STM signal involves unoccupied sample states close to the Fermi level of the tip, the new unoccupied sample states accessed at +2.5 V may dominate the signal. With a less localized and more rounded shape, the difference is explained. There is another possible, less likely, contributing factor. At +2 V, only a selection of low energy empty states contributes to the tunnel current. Thus at +2.5 V, the pentamers almost appear as spheres, because all orbitals are integrated in the STM signal. Of all the symmetries of the various states, only the rounded symmetry survives the addition of the different states. Also, considering the relatively poor resolution obtained at lower positive biases, the tip was probably in a s-type state configuration.

Fig. 1c shows a side view of the structure of the unreconstructed Si(331) surface. The green ellipse indicates the position of the pentamer after the Si(331)–(12 × 1) reconstruction is formed. The black lines indicate a nanoscale trench that runs along the $[\bar{1}10]$ direction. The Si(331)–(12 × 1) consists of alternating nano-facets oriented in the Si(111) and Si(110) directions. The alternation of these facets induces the presence of the nano-trenches. The $[\bar{1}10]$ direction is perpendicular to the direction of the double chains of pentamers of the Si(331)–(12 × 1) reconstruction. These trenches are introduced here because they will be relevant below.

We now present the structures obtained with increasing Ag coverage, below 0.3 ML and with the Si(331) substrate temperature always fixed at 600 K. Fig. 2 shows the progression with increasing coverage, starting with a large scale view with a coverage of 0.1 ML (Fig. 2a). Label 1 in Fig. 2a indicates a large trench below the level of the Si(331)–(12 × 1) reconstruction. In Fig. 2b, at a lower scale, a part of the lower intensity zones between the nanostructures is indicated by Label 2. A zoom on one of these zones is presented as an inset. In the inset, structures appearing like spheres are indicated by Label 3 in Fig. 2b. The +4 V voltage bias has been used because it is the most convenient and unambiguous way to identify the pentamers. Changing the voltage bias to +2 V allows us to confirm that these spheres correspond to the pentamers on the bare Si(331)–(12 × 1) surface. But we do not present these images. This is because, while they allowed us to identify the pentamers, their resolution was not good enough to add more information on the Ag/Si(331) system. Therefore, surviving zones of the bare surface are still present, but there is a considerable density of defects among them. Some of these defects are even one-dimensional (see Label 4 in Fig. 2b). The difficulty to image the pentamers with atomic resolution means that we cannot determine if the atomic structure of the pentamers has been affected by Ag atoms. Due to the not completely regular Ag-induced structures, it is difficult to establish the stacking and the registry with respect to the surface beneath.

In Fig. 2b, it is possible to see the formation of islands with a "sawtooth" structure. Blue dashed lines illustrate the edges of a "tooth". The back of the nanostructures is aligned along the $[\bar{1}10]$ direction, while the chains of pentamers run along the $[\bar{1}\bar{1}6]$ direction. Both directions are indicated in the figure. Ag nanostructures with a sawtooth shape were already reported on the vicinal Si(557) surface [13]. They form along the terraces of the Si(557) and have the atomic structure of the Si(111) $\sqrt{3} \times \sqrt{3}$–Ag reconstruction. Their atomic structure is thus clearly different from that of the ordered zones in our case. Another important difference is that the back edge of the "sawtooth" forms at the step edges of the Si(557) surface.

The $[\bar{1}10]$ direction is clearly a direction of preferential growth. Interestingly, it is perpendicular to the $[\bar{1}\bar{1}6]$ direction of the chains of pentamers. Therefore it is parallel to the nano-trenches described above. The tendency to form the triangular "teeth" is another indicator of organized growth. However, it is important to note that the Ag-induced structures show a lot of random variations when compared to the level of organization of model systems. More precisely, the apparent height and position of the protrusions found in the structures vary.

The main striking fact about the sawtooth nanostructures is their long and atomically straight back edge running along the $[\bar{1}10]$ direction. Even if we do not know their atomic configuration, we can propose a mechanism for their formation. The nano-trenches presented

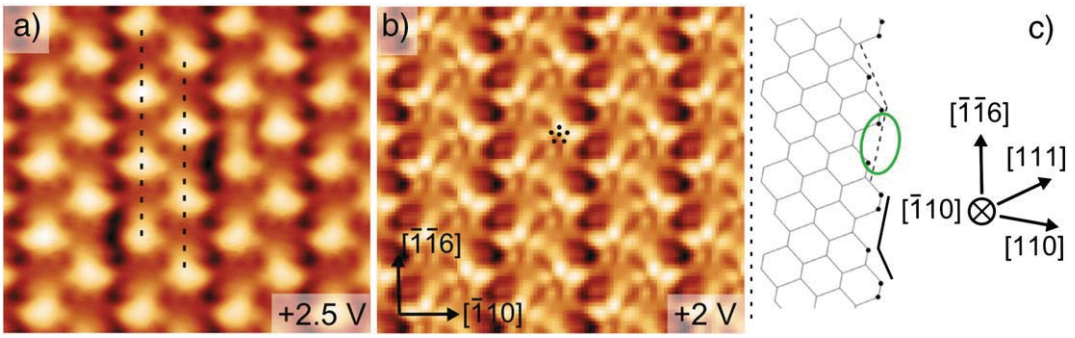

Fig. 1. Imaging of Si(331)–(12 × 1) pentamers at various voltages, 8.3 × 7.3 nm^2; a) I_{set} = 0.08 nA; b) I_{set} = 0.06 nA; the pentamers are visible in a as rounded protrusions, the chains of pentamers are highlighted by two dashed lines; in b) the positions of the outer atoms within a pentamer are highlighted by dots; c) lateral view of the model of the non-reconstructed Si(331) surface, the two black lines indicate the trench, the green ellipse the location a pentamer of the Si(331)–(12 × 1) reconstruction would occupy, crystallographic directions are also indicated; to enhance visibility in c, pentamers sites in the image are not aligned with those of a and b.

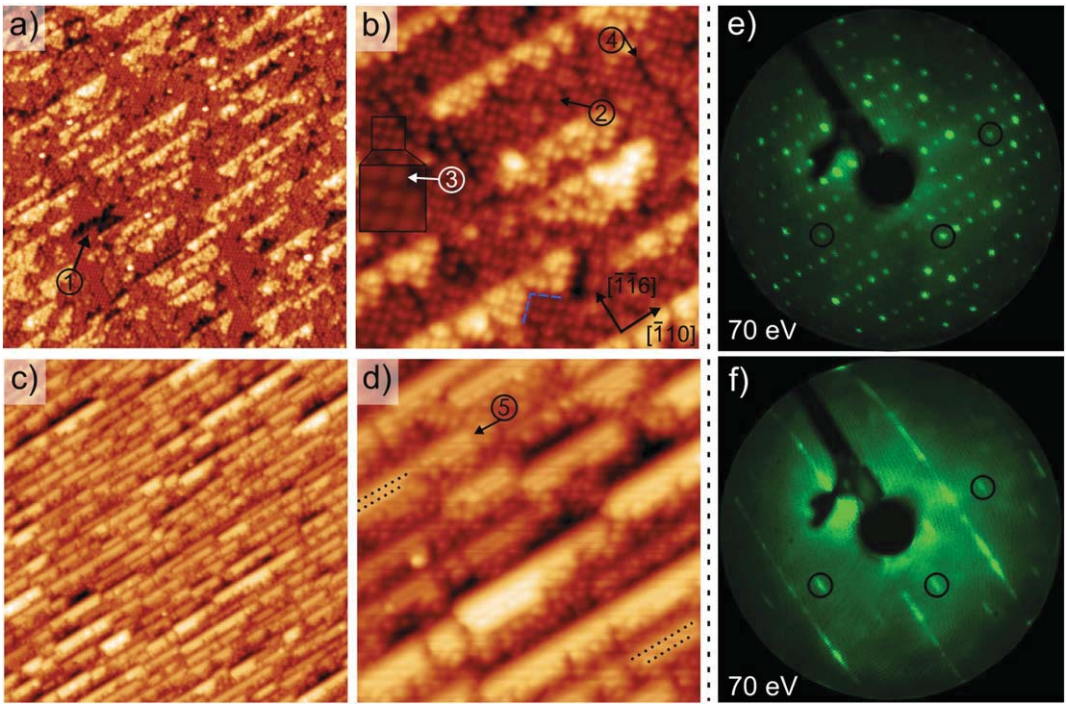

Fig. 2. Two coverages of Ag; $V_{bias} = +4$ V, $I_{set} = 0.2$ nA; a) 0.1 ML, 150×150 nm^2; b) 0.1 ML, 40×40 nm^2, the insert is a bare Si zone of 4×4 nm^2 enlarged two times, the blue dashed line highlights the "sawtooth" edges the dotted lines indicate the sub-ridges; c) 0.3 ML, 150×150 nm^2; d) 0.3 ML, 40×40 nm^2; e) LEED pattern for the bare Si(331)–(12×1) reconstruction surface; f) LEED pattern after deposition of 0.3 ML of Ag; the black circles highlight corresponding spots between the patterns; please note that the crystallographic directions were rotated with respect to Fig. 1, as indicated in b.

in Fig. 1c could provide the potential well on the surface to constrain the growth of the nanostructures. As the edges of the nanostructures, they run along the $[\bar{1}10]$ direction.

Fig. 2c shows a large scale image showing the formation of quasi-1D structures at 0.3 ML. A 40×40 nm^2 zoom is presented in Fig. 2d. In Fig. 2d, we can also observe the formation of small segments of linear structures on top of the sawtooth structures. These structures are indicated by Label 5. A division of their ridge in two sub-ridges is barely visible. The dotted lines in Fig. 2d highlight some of the segments and their two sub-ridges. Interestingly, it seems that these 1D, double-ridged segments always form close to the straight edge of the sawtooth structure. We can see, when the sawtooth structures are long enough, that the two-ridged linear structures will usually run along their whole length.

Fig. 2e and f shows the LEED patterns observed for respectively the Si(331)–(12×1) bare surface and the surface after deposition of 0.3 ML of Ag. We can see that some spots of the original Si(331)–(12×1) remain after the deposition, they are highlighted by black circles. In f, the large scale 1D ordering of the structures is clearly visible. The lines are an evidence for disorder in the perpendicular direction and order along them.

The question of whether Ag is in fact present at the surface after desorption is for now still open. In principle, it could induce changes of the surface structure before being absorbed into the Si bulk. If Ag is still present at the surface, Si atoms are likely to be incorporated in the sawtooth Ag structures. Evidence of Si migration can be seen in the large and deep triangular/sawtooth holes in the structure of pentamers, indicated by Label 1 in Fig. 2a. Fig. 2b shows that defects form in the zones of bare Si(331) surface, see Label 2. This indicates that Si atoms migrate. Overall, the apparent quantity of displaced silicon is so large, that it is almost certain that Si is present in the sawtooth structure. The question however remains open for the double-ridged segments presented in Fig. 2d.

We also tried to anneal the Ag-covered surface in order to improve order. One expects [14] a moderate annealing to increase the size of "sawtooth" zones while eliminating small irregular structures, thanks to the difference in thermal stability. The mechanism behind this is the increase of surface atoms mobility at an increased temperature.

After an annealing at 850 K for 180 s, for a Ag coverage of 0.1 ML, the surface exhibits faceting, as can be seen in Fig. 3. Determination of the angles of the facet using the STM topographic data indicates that the facets lie very close to the Si(331) direction. Angles range from approximately one to four degrees. The facets could not be associated with facets studied in literature. The facets of the type labeled as 1 in the Fig. 3a consist of micro-facets. A zoom on a facet 1 is presented in Fig. 3b, where one can see that micro-facets seem to have the pentamer Si(331)–(12×1) structure, at $V_{bias} = +4$ V. But analysis of the angles and parameter of the apparent lattice indicate that there is no match with the Si(331)–(12×1) lattice. The facets labeled as 2 seem somewhat organized but do not have the same structural properties. However, we do not have images with sufficient resolution to go further into the description. Finally, facets 3 have a disordered structure.

We can conclude that an annealing of 180 s at 850 K goes beyond the limit of the induction of faceting. The result is consistent with the findings of Dolbak et al., that the Si(331) surface breaks down in Si(111) and Si(110) facets [11], with increasing coverage and annealing temperature. However, the angles of the Si(331) surface with respect to the facets we obtained are very small compared to the angles between Si(331), Si(111) and Si(110). Faceting at low coverage means that the margin left to try to optimize the system is at least very reduced. This illustrates another type of limitation affecting the optimization of nanostructure growth. A similar effect occurs with deposition of Ag or Au on the Si(5 5 12) surface [15]. Typical other limitations include, for example, coalescence of the deposited atoms [14] and the formation of another surface reconstruction with annealing [16].

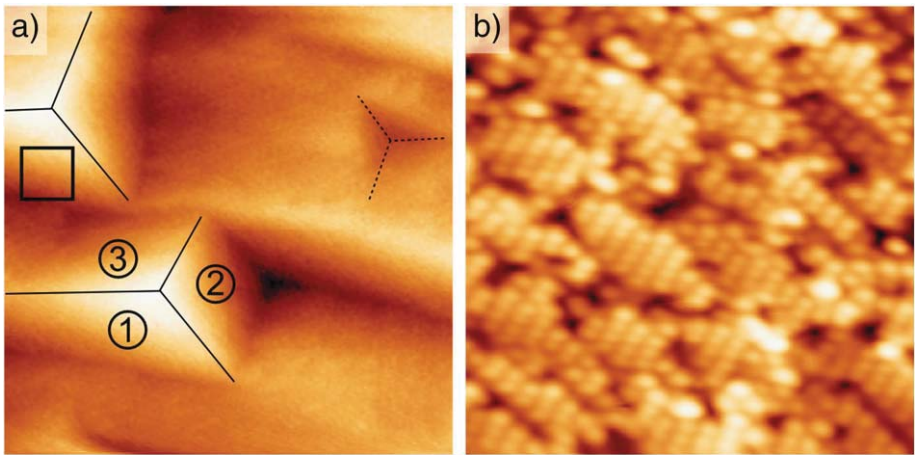

Fig. 3. STM image after deposition of 0.1 ML Ag on Si(331) and annealing at 850 K during 180 s, $V_{bias} = +4$ V, $I_{set} = 0.2$ nA; a) 200×200 nm^2 image showing the strong faceting after annealing, typical facets are labeled, the black lines highlight the edges between some facets; b) zoom on the square in the left panel, 23×23 nm^2.

4. Conclusions

We have deposited Ag on the Si(331)–(12×1) surface, at coverages below 0.3 ML to avoid faceting induced by large coverages. We have observed the formation of quasi-1D structures with sawtooth shape. Interestingly, the back edges of these structure were consistently atomically straight along the $\left[\bar{1}10\right]$ direction, without the presence of steps on the surface. They are also parallel to nano-trenches characteristic of the Si(331) unreconstructed surface. We also discuss the limits of order in this system. Annealing the surface after deposition of Ag, at a temperature of 850 K, induces faceting on the surface.

Acknowledgments

Skillful technical assistance was provided by our workshop and electronic engineering team. STM image processing was done with the programs Gwyddion and WSxM [17]. This work was supported by the Fonds National Suisse pour la Recherche Scientifique through Div. II.

References

[1] L. Du, D. Scopece, G. Springholz, F. Schäffler, G. Chen, Phys. Rev. B 90 (Aug. 2014) 075308.
[2] U. Landman, R.N. Barnett, A.G. Scherbakov, P. Avouris, Phys. Rev. Lett. 85 (Aug. 2000) 1958.
[3] F.D.M. Haldane, J. Phys. C Solid State Phys. 14 (19) (1981) 2585.
[4] J.-T. Wang, C. Chen, E. Wang, Y. Kawazoe, Phys. Rev. Lett. 105 (Sep. 2010) 116102.
[5] H. Morikawa, P.G. Kang, H.W. Yeom, Surf. Sci. 602 (24) (2008) 3745.
[6] P. Nita, G. Zawadzki, M. Krawiec, M. Jałochowski, Phys. Rev. B 84 (Aug. 2011) 085453.
[7] J.-H. Han, H.S. Kim, H.N. Hwang, B. Kim, S. Chung, J.W. Chung, C.C. Hwang, Phys. Rev. B 80 (Dec. 2009) 241401.
[8] C. Blumenstein, J. Schäfer, S. Mietke, S. Meyer, A. Dollinger, M. Lochner, X.Y. Cui, L. Patthey, R. Matzdorf, R. Claessen, Nat. Phys. 7 (2011) 776.
[9] J.M. Luttinger, J. Math. Phys. 4 (9) (1963) 1154.
[10] C. Battaglia, K. Gaál-Nagy, C. Monney, C. Didiot, E.F. Schwier, M.G. Garnier, G. Onida, P. Aebi, J. Phys. Condens. Matter 21 (1) (2009) 013001.
[11] A.E. Dolbak, B.Z. Olshanetsky, R.A. Zhachuk, Phys. Low Dimens. Struct. 7–8 (1999) 163.
[12] C. Battaglia, K. Gaál-Nagy, C. Monney, C. Didiot, E.F. Schwier, M.G. Garnier, G. Onida, P. Aebi, Phys. Rev. Lett. 102 (Feb. 2009) 066102.
[13] U. Krieg, C. Brand, C. Tegenkamp, H. Pfnür, J. Phys. Condens. Matter 25 (1) (2013) 014013.
[14] N. Mariotti, C. Didiot, E.F. Schwier, C. Monney, L.-E. Perret-Aebi, C. Battaglia, M.G. Garnier, P. Aebi, Surf. Sci. 606 (23–24) (2012) 1755.
[15] A.A. Baski, K.M. Saoud, K.M. Jones, Appl. Surf. Sci. 182 (3–4) (2001) 216 (Proceedings of the International Workshop on Nanomaterials).
[16] M.Y. Lai, Y.L. Wang, Phys. Rev. B 64 (Dec. 2001) 241404.
[17] I. Horcas, R. Fernandez, J.M. Gomez-Rodriguez, J. Colchero, J. Gomez-Herrero, A.M. Baro, Rev. Sci. Instrum. 78 (1) (2007) 013705.